

## Decay of Rabi Oscillations by Dipolar-Coupled Dynamical Spin Environments

V. V. Dobrovitski,<sup>1</sup> A. E. Feiguin,<sup>2,3</sup> R. Hanson,<sup>4</sup> and D. D. Awschalom<sup>5</sup>

<sup>1</sup>Ames Laboratory U.S. DOE, Iowa State University, Ames, Iowa 50011, USA

<sup>2</sup>Condensed Matter Theory Center, Department of Physics, University of Maryland, College Park, Maryland 20742, USA

<sup>3</sup>Microsoft Station Q, University of California, Santa Barbara, California 93106, USA

<sup>4</sup>Kavli Institute of Nanoscience Delft, Delft University of Technology, P.O. Box 5046, 2600 GA Delft, The Netherlands

<sup>5</sup>Center for Spintronics and Quantum Computation, University of California, Santa Barbara, California 93106, USA

(Received 1 April 2009; published 9 June 2009)

We study the Rabi oscillations decay of a spin decohered by a spin bath whose internal dynamics is caused by dipolar coupling between the bath spins. The form and rate of decay as a function of the intrabath coupling is obtained analytically, and confirmed numerically. The complex form of decay smoothly varies from power law to exponential, and the rate changes nonmonotonically with the intrabath coupling, decreasing for both slow and fast baths. The form and rate of Rabi oscillations decay can be used to experimentally determine the intrabath coupling strength for a broad class of solid-state systems.

DOI: 10.1103/PhysRevLett.102.237601

PACS numbers: 76.20.+q, 03.65.Yz, 76.30.-v

Measurement of the Rabi oscillations decay is an important step in studying decoherence of quantum systems. E.g., studies of Rabi oscillations in superconducting qubits damped by bosonic baths and by  $1/f$  noise [1,2] helped to extend the decoherence time to  $\mu\text{s}$  range [3], placing superconducting qubits among most promising solid-state candidates. Recently, much progress has been achieved in experimental implementation of long-living coherent Rabi oscillations in various spin systems: magnetic molecules [4], NV impurity centers in diamond [5–7], rare-earth ions in host crystals [8], quantum dots [9–11]. Many of these systems are attractive for basic studies of quantum spin coherence effects, and show much promise for quantum information processing, coherent spintronics, or high-precision magnetometry, provided that detailed understanding of the decoherence processes will be achieved.

A major decoherence source in these spin systems is the coupling of the central spin (e.g., the electron spin of the NV center) to other spins in the sample (environmental bath spins, e.g., the spins of nitrogen atoms in diamond). Moreover, for many relevant spin systems, the direct coupling between the environmental spins is essential, producing internal dynamics of the bath. Here we explore theoretically the influence of such a dynamical spin bath on the Rabi oscillations of the central spin. Avoiding the commonly used framework of generalized Bloch equations [12–15], we are able to investigate the form and rate of decay as a function of the intrabath coupling strength. We find interesting behavior of the Rabi oscillations, which contradicts the expectations based on standard Redfield-type analysis: e.g., the slow bath leads to pronounced decay, while for the fast bath the decay rate vanishes but the Rabi frequency becomes renormalized. We demonstrate how the form and rate of the Rabi oscillations decay can be used to experimentally characterize the intrabath dynamics, and provide a rather simple recipe for analysis of data.

We focus on dilute dipolar-coupled bath: in a nonmagnetic crystal, a single central spin of species  $S$  (e.g., a paramagnetic impurity) is coupled to a bath of dilute spins of species  $I$  (e.g., other kind of paramagnetic impurities, or nuclear spins). The coupling between the bath spins is non-negligible, and is caused by dipolar interactions. This situation encompasses a wide range of interesting solid-state spin systems, from Er ions in  $\text{CaWO}_4$  studied in 1960s [16] to the NV centers in diamond [5–7] which gained much attention recently. The NV centers may be particularly suitable for detailed studies of Rabi oscillations and verification of the model due to possibility of optical readout of a single central spin [17], and tunable spin bath made of surrounding nitrogen atoms [7].

We assume that a very large magnetic field  $B_z$  is applied along the  $z$  axis (as in standard NMR/ESR settings), leading to Zeeman splittings  $\omega_S = \gamma_S B_z$  for the central spin  $S$  and  $\omega_I = \gamma_I B_z$  for the bath spins  $I_k$  ( $\gamma_S$  and  $\gamma_I$  are the gyromagnetic ratios of the  $S$  and  $I$  spins, respectively). Also, strong Rabi driving field  $H_R$  is applied at the frequency  $\omega_S$ . The difference  $|\omega_S - \omega_I|$  is much larger than any other energy scale, so the mutual flips of the central spin and the bath spins involve huge Zeeman energy mismatch and are strongly suppressed. Hence, the terms like  $S^+ I_k^-$  become irrelevant on a time scale of Rabi oscillations decay (see below); omitting these terms and transforming into rotating frame we obtain a secular Hamiltonian [12,13]:

$$H = h_x S_x + \sum_k A_k S_z I_k^z + \sum_{k,l} C_{kl} (3I_k^z I_l^z - \mathbf{I}_k \cdot \mathbf{I}_l), \quad (1)$$

where  $S^{x,y,z}$  and  $I_k^{x,y,z}$  are the spin operators in the rotating frame, and  $h_x = H_R/2$  is the rotating-frame Rabi driving field. The coupling constants  $A_k = \gamma_S \gamma_I [1 - 3(n_k^z)^2]/r_k^3$  are determined by the positions  $\mathbf{r}_k$  of the bath spins  $I_k$  ( $k = 1, \dots, N$ ), where  $r_k = |\mathbf{r}_k|$  and  $\mathbf{n}_k = \mathbf{r}_k/r_k$  (the origin of the coordinate frame coincides with the central spin). Simi-

larly, the intrabath couplings  $C_{kl} = \gamma_i^2[1 - 3(n_{kl}^z)^2]/r_{kl}^3$  are determined by the vectors  $\mathbf{r}_{kl} = \mathbf{r}_k - \mathbf{r}_l$ . Note that the same Hamiltonian (1) can be obtained without external field  $B_z$  if the transition frequencies  $\omega_S$  and  $\omega_I$  are determined by the zero-field splitting (e.g., due to anisotropic interactions). Similarly, the assumption (used below) that  $S$  and  $I_k$  are spins 1/2 is not essential: for larger spins, we can consider each pair of levels as a pseudospin 1/2 [12,13].

Initially the central spin is in the state “up,” and the bath is in a maximally mixed state (unpolarized bath at high temperatures); i.e., the initial density matrix of the whole system is  $\rho(0) = 2^{-N}|\uparrow\rangle\langle\uparrow| \otimes \mathbf{1}_B$ , where  $\mathbf{1}_B$  is the  $2^N \times 2^N$  identity matrix. This is appropriate for most experiments (for nuclear spins at temperatures above a few nK, for electron spins—above tens of K). We calculate the time-dependent  $z$  component of the central spin  $\langle S_z(t) \rangle = \text{Tr}\rho(t)S_z$ , where  $\rho(t) = \exp(-iHt)\rho(0)\exp(iHt)$ . In order to see well-pronounced long-living Rabi oscillations, the driving field should be large, so we assume that  $h_x$  is much larger than all other energy scales [18]. We calculate the oscillations damping in the lowest order in  $1/h_x$ , treating the second (spin-bath coupling) and the third (bath internal Hamiltonian) terms in Eq. (1) perturbatively, and excluding the bath internal Hamiltonian  $H_B = \sum_{k,l} B_{kl}(3I_k^z I_l^z - \mathbf{I}_k \cdot \mathbf{I}_l)$  by the interaction representation transformation. The resulting second-order Hamiltonian

$$H_0 = h_x S_x + S_x \hat{B}^2(t)/(2h_x), \quad (2)$$

where  $\hat{B}(t) = \exp(iH_B t)\hat{B}\exp(-iH_B t)$ , and the operator  $\hat{B} = \sum_k A_k I_k^z$ .

The evolution of  $\hat{B}(t)$  is complex, involving intricate correlations between bath spins. However, exact dynamics of every single bath spin is not important, since  $\langle S_z(t) \rangle$  involves tracing over all bath spins. This is typical for many spin-bath decoherence problems, from magnetic resonance to quantum information processing, and many approaches have been developed from the early days of NMR/ESR theory [19,20] till very recently [21–28]. Below, following the works [19,20], we approximate the effect of the bath by a random field  $B(t)$ , which is modeled as an Ornstein-Uhlenbeck process with the correlation function  $\langle B(t)B(0) \rangle = b^2 \exp(-Rt)$ , where the dispersion  $b = \sqrt{\sum_k A_k^2}$ , while the correlation decay rate  $R$  is determined by  $H_B$ . This model may be oversimplified for complicated situations, e.g., the description of advanced control protocols requires more sophisticated treatment [23,24,28]. However, our direct numerical simulations evidence that this model is *quantitatively* adequate for description of the Rabi oscillations decay, while providing a clear description of the physics underlying the Rabi oscillations decay, and allowing access to the regimes outside of the Bloch equations framework.

The Hamiltonian (2) reflects a simple physical picture. The zero-order eigenstates of the Hamiltonian (1) correspond to the central spin states  $|+\rangle = 1/\sqrt{2}[|\uparrow\rangle + |\downarrow\rangle]$  and

$|-\rangle = 1/\sqrt{2}[|\uparrow\rangle - |\downarrow\rangle]$ , separated by a large Rabi frequency  $h_x$ . Since  $h_x \gg b$  and  $h_x \gg R$ , the field  $B(t)$  has no spectral components of noticeable magnitude at the Rabi frequency, and does not lead to transition between the states  $|+\rangle$  and  $|-\rangle$ . The only relevant process is the pure dephasing, when the field  $B$  destroys the initial phase relation between the states  $|+\rangle$  and  $|-\rangle$ , leading to decay of  $\langle S_z(t) \rangle$ , so that

$$\langle S_z(t) \rangle = 1/2 \langle \cos\Phi \rangle = 1/2 \text{Re}\langle \exp(i\Phi) \rangle, \quad (3)$$

where  $\langle \cdot \rangle$  denotes average over all possible realizations of  $B(t)$ , and the phase

$$\Phi = h_x t + \frac{1}{2h_x} \int_0^t B^2(s) ds = h_x t + \Theta \quad (4)$$

is the total phase difference between the states  $|+\rangle$  and  $|-\rangle$  accumulated during time  $t$ , cf. the Hamiltonian (2). The key quantity  $M(t) = \langle \exp(i\Theta) \rangle$  is an analytically computable Gaussian path integral over the Ornstein-Uhlenbeck process, which gives the answer

$$\begin{aligned} \langle S_z(t) \rangle &= 1/2 \text{Re}[M(t) \exp(ih_x t)] \\ [M(t)]^{-2} &= \exp(-Rt) [\cosh Pt + (R/P) \sinh Pt] \\ &\quad - i \frac{b^2}{h_x P} \exp(-Rt) \sinh Pt, \end{aligned} \quad (5)$$

where  $P = \sqrt{R^2 - 2ib^2R/h_x}$ .

Analysis of Rabi oscillations is often based on Bloch-type equations [12] or its generalizations [14], derived for various systems from quantum optics [15] to solid state [14]. It is based on the Redfield-type approach [12,13], taking into account only the terms which are secular with respect to the Rabi driving  $h_x S_x$ . In addition to dephasing, these terms describe the actual transitions between the states  $|+\rangle$  and  $|-\rangle$ , which lead to a longitudinal relaxation (along the  $x$  axis) of the central spin with the rate  $\Gamma_l \sim b^2 R/h_x^2$ . This rate is of second order in  $1/h_x$ , and is determined by the spectral density of  $B(t)$  at the Rabi frequency  $h_x$ . Also, the generalized Bloch equations, having constant coefficients, always predict the decay to have a (multi)exponential form. In contrast, our results are not limited to the terms secular with respect to Rabi driving, and give the decay rate of the first order in  $1/h_x$ . The solution (5) predicts the decay which has, in general, no simple form (multiexponential, Gaussian, power law, etc.) The familiar exponential decay occurs only at special values of  $b$ ,  $h_x$ , and  $R$ , see below.

The effect of the bath internal dynamics may be important even for slow baths, with  $R \ll b^2/h_x$ . In this limit,  $P = b\sqrt{-2iR/h_x}$ , see Eq. (5). At short times  $t \ll 1/|P|$ , the bath behaves as static, and the Rabi oscillations envelope exhibits nonexponential slow decay of the form  $[1 + (b^2 t/h_x)^2]^{-1/4}$ , in accordance with the exact results obtained earlier [9,25–27]. At long times  $t \gg 1/|P|$ , the decay has exponential form  $\exp(-bt\sqrt{R/4h_x})$ , with the rate which decreases very slowly with decreasing  $R$ . As a result, even for very slow bath the effect of the bath

dynamics remains noticeable. In experiments, the above-described behavior of the Rabi oscillations decay can be detected by varying  $h_x$  (since the ratio of  $R$  to  $b^2/h_x$  determines how fast or slow the bath is), and makes it possible to estimate  $b$  and  $R$ .

Another interesting feature of our results is that the decay of Rabi oscillations changes nonmonotonically with  $R$ : it is fastest for  $R \sim b^2/h_x$ , slowing down for both slow and fast baths. This is confirmed by direct numerical simulations, see Fig. 1 and discussion below.

The regime of fast bath, with  $R \gg b^2/h_x$ , is even more interesting and unexpected. In this case

$$M(t) = \exp\left[i\frac{b^2 t}{2h_x} - \frac{b^4 t}{4h_x^2 R}\right], \quad (6)$$

and the Rabi oscillations exhibit exponential decay with the rate  $\Gamma_t = b^4/(4h_x^2 R)$ , which vanishes quickly for large  $R$ . However, it does not mean that the effect of the fast bath disappears. The bath still noticeably affects the central spin, shifting its Rabi frequency by  $b^2/2h_x$ , and only the decaying part of the bath effect vanishes [29]. This slowing of the Rabi oscillations decay is confirmed by direct numerical simulations (Fig. 2).

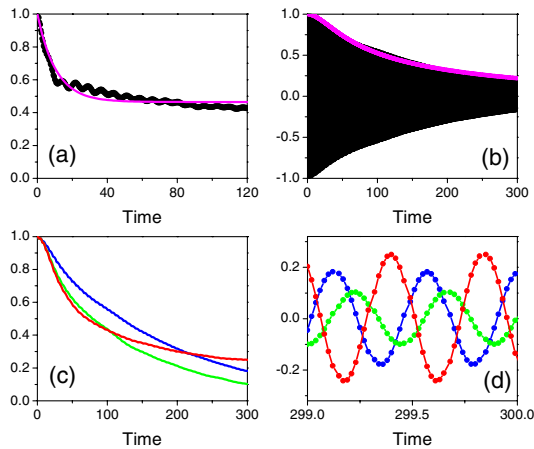


FIG. 1 (color online). Exact simulations for  $N = 15$  bath spins. (a) Correlation function  $C(t) = (1/b^2)\langle B(0)B(t) \rangle$  (normalized by  $b^2$ ) obtained from direct simulations (black), see also [31]. Its fitting (magenta or gray) determines the bath parameters  $b_1$ ,  $b_2$ , and  $R$  for each value of the intrabath coupling scale  $E_B$  (here  $E_B = 1$ ,  $b_1 = 0.62$ ,  $b_2 = 0.58$ ,  $R = 0.095$ ). (b) Rabi oscillations decay for  $h_x = 14.14$ ,  $b = 0.85$ , and  $E_B = 1$ ; individual oscillations are not resolved. Numerics (black) agrees well with analytics (magenta, only the envelope shown). (c) Envelopes of simulated Rabi decay for  $E_B = 1$  (blue or dark gray), 0.1 (green or light gray), and 0 (static bath, red or gray); corresponding individual oscillations near  $t = 300$  are shown on panel (d) by the same colors. Analytical results practically coincide with simulations, and are not shown. The decay rate changes nonmonotonically with  $E_B$ : the decay is slower for  $E_B = 1$  (blue) and 0 (red) in comparison with  $E_B = 0.1$  (green). At  $t = 300$ , on panel (d), the oscillation amplitude for  $E_B = 0.1$  (green) is twice smaller than that for  $E_B = 0$ .

On the other hand, for fast baths, the transitions between the states  $|+\rangle$  and  $|-\rangle$  become important. While the dephasing between these states just shifts the Rabi frequency, the transitions lead to longitudinal relaxation along the  $x$  axis with the rate  $\Gamma_l \sim b^2 R/h_x^2$ . This implies [12] exponential decay of Rabi oscillations with the rate  $\Gamma_l/2$ , which is comparable with the decay rate  $\Gamma_l$  caused by the pure dephasing. Above, for simplicity, we omitted the longitudinal relaxation (since it is of order  $1/h_x^2$ ), but we can include it using the Redfield-type approach: the answer (5) for  $S_z(t)$  just has to be multiplied by  $\exp(-\Gamma_l t/2)$ . This explains how the system enters the generalized Bloch equation regime at  $R \gg b$ : the dephasing effect becomes negligible and the longitudinal relaxation becomes dominant. In experiment, this regime can be identified by comparing  $\Gamma_l$  and  $\Gamma_i$ ; they would be of the same order, changing as  $1/h_x^2$  for all sufficiently large  $h_x$ .

To ensure that the physical picture above is adequate for real dipolar-coupled bath, we performed direct numerical simulations of the Rabi oscillations decay. We place the central spin and  $N$  bath spins randomly, with uniform den-

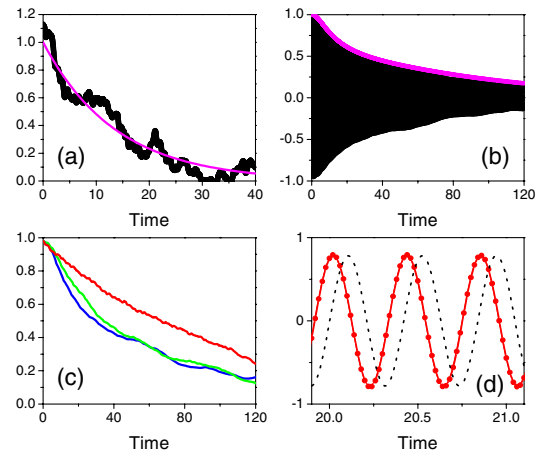


FIG. 2 (color online). Numerical simulations for  $N = 159$  bath spins. (a) Correlation function  $C(t) = (1/b^2)\langle B(0)B(t) \rangle$  (normalized by  $b^2$ ) obtained from  $P$ -representation sampling simulations (black); its fitting (magenta or gray) determines the parameter  $R$  for each value of the intrabath coupling scale  $E_B$  (here  $E_B = 1$  and  $R = 0.097$ ). In spite of noticeable statistical fluctuations [e.g.,  $C(0)$  is slightly larger than 1 due to them], the parameter  $R$  is determined precisely enough to be used in Eq. (5). (b) Rabi oscillations decay for  $h_x = 15.0$ ,  $b = 1.39$ , and  $E_B = 0.1$ ; individual oscillations are not resolved. Numerics (black) agrees well with analytics (magenta, only the envelope shown). (c) Envelopes of simulated Rabi decay for  $E_B = 0.1$  (blue or dark gray), 1 (green or light gray), and 10 (red or gray); the longitudinal decay for  $E_B = 10$  is taken into account. Analytical results practically coincide with simulations, and are not shown. The decay rate decreases for faster baths: the decay is slowest for  $E_B = 10$  (red). Individual oscillations for  $E_B = 10$  near  $t = 20$  are shown on panel (d) in red: their frequency is shifted by  $b^2/2h_x = 0.064$  from the value  $h_x = 15.0$  (oscillations with frequency  $h_x = 15.0$  are shown by dotted black line to demonstrate the phase difference accumulated since  $t = 0$ ).

sity  $n = 1$ , inside a cube with the side  $(N + 1)^{1/3}$ , central spin being in the center of the cube. All interaction coefficients are calculated according to Eq. (1), using the actual coordinates of the spins. The value  $E_{SB} = \gamma_S \gamma_I$ , which determines the strength of coupling between the central spin and the bath, is set to 1, thus defining the energy and time scales for all quantities below. The value  $E_B = \gamma_I^2$ , which governs the energy scale of intrabath couplings, is varied, making the bath slower or faster. We simulate the dynamics of the system using two numerical approaches. For small  $N$  (e.g.,  $N = 15$  in Fig. 1) we exactly solve of the Schrödinger equation with the Hamiltonian (1) via Chebyshev polynomial expansion [30]. The dipolar-coupled systems with  $N > 15$  are difficult to model this way (due to exponentially increasing resources requirements), so we use the  $P$ -representation sampling [30] for modeling larger baths ( $N = 159$  in Fig. 2). To compare numerical solutions with the analytics, we calculate the total coupling to a bath  $b = [\sum_{k=1}^N A_k^2]^{1/2}$  directly from the positions of the spins [see Eq. (1) and below]. The correlation decay rate  $R$  requires a separate simulation: we calculate  $\langle B(0)B(t) \rangle$  and find  $R$  by fitting it to a decaying exponent, see also [31]. Varying the system parameters in a wide range, we simulated baths with  $N = 15, 59$ , and 159 spins, and found good agreement between numerics and analytics; typical results are given in Figs. 1 and 2.

The resulting experimental recipe is rather simple. If the decay has a power law form at shorter times, changing to exponent later, with the decay constants changing as  $1/h_x$  and the duration of the two regimes varying with  $h_x$ , then the bath is slow. If the Rabi oscillations decay is exponential, with the rate changing as  $1/h_x^2$  and the frequency shift varying as  $1/h_x$ , then the bath is fast. The fast bath can be made slow by strong increase in  $h_x$ .

Summarizing, we studied the decay of the Rabi oscillations of the central spin interacting with a dipolar-coupled dynamical spin bath. Approximating the effect of the bath as a random field (Ornstein-Uhlenbeck process), we find analytically the form of the decay. Validity of the approximation is confirmed by direct numerical simulations. The oscillations decay has interesting features, such as nonmonotonic variation of the decay rate with increasing the intrabath coupling, and slowing down of the decay for fast baths. Studying the Rabi oscillations decay may help in experimental characterization of the dynamical spin bath, and is well within experimental reach, e.g., for NV centers in diamond.

Work at Ames Laboratory was supported by the Department of Energy—Basic Energy Sciences under Contract No. DE-AC02-07CH11358. We acknowledge support from AFOSR (D. D. A.), FOM and NWO (R. H.). A. E. F. acknowledges support from the Microsoft Corporation.

- [2] J. Clarke and F. K. Wilhelm, *Nature (London)* **453**, 1031 (2008).
- [3] G. Ithier *et al.*, *Phys. Rev. B* **72**, 134519 (2005); A. A. Houck *et al.*, *Phys. Rev. Lett.* **101**, 080502 (2008).
- [4] S. Bertaina *et al.*, *Nature (London)* **453**, 203 (2008).
- [5] T. Gaebel *et al.*, *Nature Phys.* **2**, 408 (2006).
- [6] L. Childress *et al.*, *Science* **314**, 281 (2006).
- [7] R. Hanson *et al.*, *Science* **320**, 352 (2008).
- [8] S. Bertaina *et al.*, *Nature Nanotech.* **2**, 39 (2007).
- [9] F. H. L. Koppens *et al.*, *Phys. Rev. Lett.* **99**, 106803 (2007).
- [10] J. R. Petta *et al.*, *Science* **309**, 2180 (2005).
- [11] R. Hanson *et al.*, *Rev. Mod. Phys.* **79**, 1217 (2007).
- [12] C. P. Slichter, *Principles of Magnetic Resonance* (Springer, Berlin, New York, 1990).
- [13] A. Abragam, *Principles of Nuclear Magnetism* (Oxford University Press, Oxford, New York, 1961).
- [14] E. Geva *et al.*, *J. Chem. Phys.* **102**, 8541 (1995).
- [15] C. Cohen-Tannoudji and S. Reynaud, *J. Phys. B* **10**, 365 (1977).
- [16] W. B. Mims, *Phys. Rev.* **168**, 370 (1968).
- [17] F. Jelezko *et al.*, *Phys. Rev. Lett.* **92**, 076401 (2004).
- [18] For a static bath prepared with a well-defined value of  $B$ , the Rabi oscillations do not decay even for small  $h_x$ . However, the majority of typical experiments involves averaging over  $B$ , implied by the initial maximally mixed state of the bath.
- [19] P. W. Anderson and P. R. Weiss, *Rev. Mod. Phys.* **25**, 269 (1953); J. R. Klauder and P. W. Anderson, *Phys. Rev.* **125**, 912 (1962).
- [20] R. Kubo, *J. Phys. Soc. Jpn.* **17**, 1100 (1962).
- [21] A. Garg, *Phys. Rev. Lett.* **74**, 1458 (1995).
- [22] V. V. Dobrovitski *et al.*, *Phys. Rev. Lett.* **90**, 210401 (2003).
- [23] W. A. Coish and D. Loss, *Phys. Rev. B* **72**, 125337 (2005).
- [24] R. de Sousa and S. Das Sarma, *Phys. Rev. B* **68**, 115322 (2003); W. M. Witzel and S. Das Sarma, *Phys. Rev. B* **74**, 035322 (2006).
- [25] V. V. Dobrovitski *et al.*, quant-ph/0112053; *HAIT J. Sci. Eng.* **1**, 586 (2005).
- [26] F. M. Cucchietti *et al.*, *Phys. Rev. A* **72**, 052113 (2005).
- [27] J. M. Taylor and M. D. Lukin, *Quant. Info. Proc.* **5**, 503 (2006).
- [28] W. Yao *et al.*, *Phys. Rev. Lett.* **98**, 077602 (2007); S. Saikin *et al.*, *Phys. Rev. B* **75**, 125314 (2007).
- [29] This is in clear contrast with the motional narrowing phenomenon, when the free oscillations decay rate vanishes for fast bath [12,13,19,20]. In the motional narrowing case, extremely fast bath does not affect the central spin at all.
- [30] W. Zhang *et al.*, *J. Phys. Condens. Matter* **19**, 083202 (2007).  $P$ -representation sampling, although not exact, is expected to give accurate results for our problem at large  $N$ .
- [31] For  $N = 15$ , due to finite- $N$  effects, the correlations decay to a finite value, so that the field  $B(t)$ , in addition to the Ornstein-Uhlenbeck component, has a static component (of the order of  $1/\sqrt{N}$ ), and the correlation function has the form  $\langle B(0)B(t) \rangle = b_1^2 \exp(-Rt) + b_2^2$ , with restriction  $b_1^2 + b_2^2 = b^2$ .

[1] Y. M. Galperin *et al.*, *Phys. Rev. Lett.* **96**, 097009 (2006).